

Generating continuous variable quantum codewords in the near-field atomic lithography

Stefano Pirandola, Stefano Mancini, David Vitali, and Paolo Tombesi

*INFM, Dipartimento di Fisica, Università di Camerino,
via Madonna delle Carceri, I-62032 Camerino, Italy*

(Dated: September 18, 2017)

Recently, D. Gottesman *et al.* [Phys. Rev. A **64**, 012310 (2001)] showed how to encode a qubit into a continuous variable quantum system. This encoding was realized by using non-normalizable quantum codewords, which therefore can only be approximated in any real physical setup. Here we show how a neutral atom, falling through an optical cavity and interacting with a single mode of the intracavity electromagnetic field, can be used to safely encode a qubit into its external degrees of freedom. In fact, the localization induced by a homodyne detection of the cavity field is able to project the near-field atomic motional state into an approximate quantum codeword. The performance of this encoding process is then analyzed by evaluating the intrinsic errors induced in the recovery process by the approximated form of the generated codeword.

PACS numbers: 03.67.Pp, 03.75.Be, 42.50.Vk, 42.50.St

I. INTRODUCTION

During last years quantum information and computation have been extended to the continuous variable (CV) framework [1]. In this framework, quantum and classical information is encoded and processed using quantum systems, like oscillators and particles, which are described by observables with a continuous spectrum of eigenvalues. Recently, also quantum error correction (QEC) has been extended to this framework, in order to allow a reliable CV quantum computation [2, 3]. In fact, as shown in Ref. [3], a whole class of CV QEC codes can be designed to fight the effects of decoherence over a set of particles, the most probable effect being a small diffusion in the position and momentum of all the particles. These codes have been suitably derived by extending to CV systems the *shift-resistant* quantum codes for qudits, and they can be used to implement an universal set of fault-tolerant quantum gates [3]. However, the main drawback of the CV QEC seems to be the physical preparation of the quantum codewords. In fact, these codewords ideally are non-normalizable states (since superpositions of infinitely squeezed states) and, in any real physical implementation, they can only be approximated by normalizable states, which will consequently introduce intrinsic errors in the recovery process. Some literature has been devoted to the development of schemes and techniques able to reduce the intrinsic error probability in the recovery process. In particular, Ref. [4] has resorted to a sequence of operations similar to a quantum random walk algorithm [5]. More recently, we have proposed an all-optical scheme, based on the cross-Kerr interaction [6], and a trapped ion scheme [7], based on a ponderomotive interaction [8].

Here, revisiting some results of Refs. [9] and [10] on atomic lithography, we show how to embed a qubit in the external degrees of freedom of a free neutral atom. As in Ref. [9], we consider a two-level atom passing through an optical cavity and interacting with a single mode of the intracavity electromagnetic field. Then, by making a quadrature phase measurement on the field, it is possible to localize the position of the atom within the wavelength of the light in the cavity which acts as a virtual diffraction grating. Depending on the initial state, the field measurement may localize the atomic position wavefunction into one or more virtual slits. In particular, we are interested in the case of an input state sufficiently delocalized in position, so that the measurement-induced localization of the atom will result in the generation of a comb-like state, which represents the finite-energy approximation of an ideal CV quantum codeword.

The paper is organized as follows. In Sec. II we rapidly review some elements from Ref. [3] and we turn from an ideal situation to a more realistic one. In Sec. III the physical implementation of the encoding scheme is proposed. Sec. IV is for conclusions.

II. CONTINUOUS VARIABLE QUANTUM CODEWORDS

A single qubit living in a Hilbert space \mathcal{H} with basis $\{|0\rangle, |1\rangle\}$ can be encoded into a single particle [11] in such a way that the two resulting codewords $|\overline{0}\rangle, |\overline{1}\rangle$ provide protection against small diffusion errors in both position x and momentum p (the quantum operators obey the commutation rule $[\hat{x}, \hat{p}] = i$ so that x, p are dimensionless quantities). The two quantum codewords $|\overline{0}\rangle, |\overline{1}\rangle$ are the simultaneous eigenstates, with eigenvalue +1 of the displacement operators

$\hat{D}_x(2\theta)$, $\hat{D}_p(2\pi\theta^{-1})$ with $\theta \in \mathbb{R}$, which are also the stabilizer generators of the code [12]. These codewords are therefore invariant under the shifts $x \rightarrow x - 2\theta$ and $p \rightarrow p - 2\pi\theta^{-1}$. Up to a normalization factor they are given by

$$|\overline{0}\rangle = \sum_{s=-\infty}^{+\infty} |x = 2\theta s\rangle = \sum_{s=-\infty}^{+\infty} |p = \pi\theta^{-1}s\rangle \quad (1)$$

$$|\overline{1}\rangle = \sum_{s=-\infty}^{+\infty} |x = 2\theta s + \theta\rangle = \sum_{s=-\infty}^{+\infty} (-1)^s |p = \pi\theta^{-1}s\rangle = \hat{D}_x(\theta)|\overline{0}\rangle \quad (2)$$

i.e. they are a coherent superposition of infinitely squeezed states (position eigenstates and momentum eigenstates). Each of them is a comb-state both in x and in p with equally spaced spikes (2θ in x and $\pi\theta^{-1}$ in p). The codewords $|\overline{0}\rangle, |\overline{1}\rangle$ are also eigenstates of the encoded bit-flip operator $\bar{Z} = \hat{D}_p(\pi\theta^{-1})$. Equivalently one can also choose the codewords $|\overline{\pm}\rangle = [|\overline{0}\rangle \pm |\overline{1}\rangle]/\sqrt{2}$ which are the eigenstates of the encoded phase-flip operator $\bar{X} = \hat{D}_x(\theta)$ and are given by:

$$|\overline{+}\rangle = \sum_{s=-\infty}^{+\infty} |x = \theta s\rangle = \sum_{s=-\infty}^{+\infty} |p = 2\pi\theta^{-1}s\rangle \quad (3)$$

$$|\overline{-}\rangle = \sum_{s=-\infty}^{+\infty} (-1)^s |x = \theta s\rangle = \sum_{s=-\infty}^{+\infty} |p = 2\pi\theta^{-1}s + \pi\theta^{-1}\rangle. \quad (4)$$

Also these states are comb-like states both in x and in p , with equally spaced spikes (θ in x and $2\pi\theta^{-1}$ in p). The four codewords states are schematically displayed in Fig. 1.

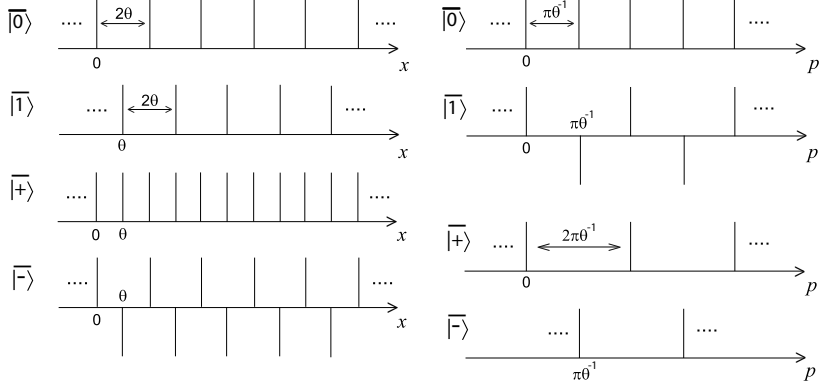


FIG. 1: Ideal encoded states $|\overline{0}\rangle, |\overline{1}\rangle$ (\bar{Z} eigenstates) and $|\overline{+}\rangle, |\overline{-}\rangle$ (\bar{X} eigenstates). On the left the structure of the spatial wavefunctions is displayed while on the right the structure of the momentum wavefunction is displayed. Each spike is ideally a Dirac-delta function.

The recovery process is realized by measuring the stabilizer generators $\hat{D}_x(2\theta), \hat{D}_p(2\pi\theta^{-1})$. The measurement of the X -generator $\hat{D}_x(2\theta) = e^{-i2\theta\hat{p}} = \hat{p}(\text{mod}\pi\theta^{-1})$ reveals momentum shifts Δp which are correctable if $|\Delta p| < \pi\theta^{-1}/2$; in such a case the correction is made by shifting p so to become equal to the nearest multiple of $\pi\theta^{-1}$. In the same way, the measurement of the Z -generator $\hat{D}_p(2\pi\theta^{-1}) = e^{i2\pi\theta^{-1}\hat{x}} = \hat{x}(\text{mod}\theta)$ reveals position shifts which are correctable if $|\Delta x| < \theta/2$; in such a case the correction is made by shifting x so to coincide with the nearest multiple of θ .

Ref. [3] proposed the following recipe for the generation of the codeword states.

1. Preparation of a particle in the $p = 0$ eigenstate (i.e. completely delocalized in position).
2. Coupling the particle to a meter (i.e. an oscillator, with ladder operators \hat{c}, \hat{c}^\dagger) via the non linear interaction $\hat{H}_{NL} = g\hat{c}^\dagger\hat{c}\hat{x}$. This interaction modifies the frequency of the meter by $\Delta\omega = gx$ so that, at time $t = \pi\theta^{-1}g^{-1}$, the phase of the meter is shifted by $\Delta\phi = \pi\theta^{-1}x$.
3. Reading out the phase of the meter $\Delta\phi$ at a time t , i.e. measuring $\hat{x}(\text{mod}2\theta)$. This measurement projects the initial state into a superposition of equally spaced delta function $\delta(x - 2\theta s + \varepsilon)$ with $s = 0, \pm 1, \dots$ and $\varepsilon \in \mathbb{R}$.

4. Applying a suitable transformation to obtain any desired encoded qubit state $a|\overline{0}\rangle + b|\overline{1}\rangle$.

Ideally the codewords are non-normalizable states infinitely squeezed both in x and p , but in practice one can only generate states with finite squeezing, i.e. only approximate codewords: $|\overline{0}\rangle \sim |\overline{0}\rangle$, $|\overline{1}\rangle \equiv \hat{D}_x(\theta)|0\rangle \sim |\overline{1}\rangle$, $|\overline{\pm}\rangle \equiv [|\overline{0}\rangle \pm |\overline{1}\rangle]/\mathcal{N}_{\pm} \sim |\overline{\pm}\rangle$ (\mathcal{N}_{\pm} are normalization constants). For this reason, in order to estimate the quality of the encoding scheme, together with the error probability in the recovery process due to the occurrence of an uncorrectable error, we have also to consider the *intrinsic error probability* due to the imperfections of the approximate codewords which can lead to an error even in the presence of a correctable error. Here we propose a physical implementation of the ideal coding protocol of Ref. [3] based on single neutral atoms interacting with a radiation mode. It can be derived from the ideal one by replacing the initial $p = 0$ state with a finitely squeezed state, \hat{H}_{NL} with a ponderomotive interaction, and the phase measurement with a homodyne measurement.

III. ENCODING BY ATOMIC LITHOGRAPHY

Our scheme concerns a two-level atom transversally crossing a high finesse optical cavity and interacting with one of its modes (see Fig. 2 for a schematic description). We shall see that, if at an appropriate interaction time a homodyne measurement of an intracavity quadrature is performed, the center-of-mass motion of the atom is projected onto an approximate comb-like state, which can be used for the generation of the approximated codeword states. Notice that here we are encoding a qubit into the external degrees of freedom of a *free* atom, which can be always seen as a quantum oscillator with zero frequency.

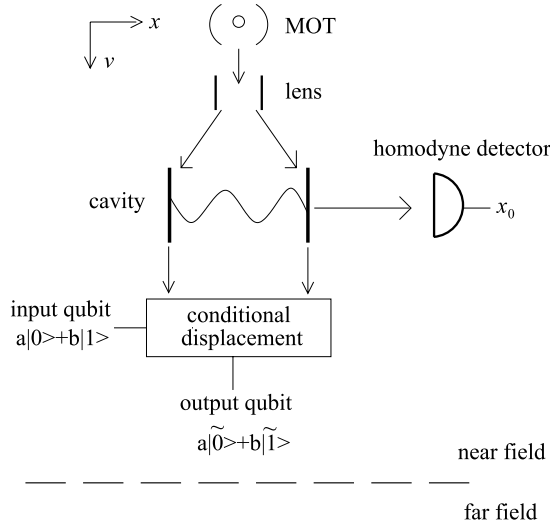


FIG. 2: An atom cooled in a MOT freely falls through a high finesse cavity, orthogonally to the cavity axis. Above the cavity (and relatively far from it) a diverging atomic lens causes a delocalization of the atomic wave-function entering the cavity. The atom interacts with a single mode of the cavity and after a suitable interaction time, the intracavity quadrature $\hat{x}_0 = \hat{c} + \hat{c}^\dagger$ is measured and the atomic wave-function is projected onto an approximate comb-like state, which we take as the approximate codeword $|\overline{0}\rangle$. A conditional displacement (see text) can then be used to generate any correctable state $a|\overline{0}\rangle + b|\overline{1}\rangle$.

This set-up can be realized using a small sample of atoms cooled in a magneto-optical-trap (MOT) [13] placed above the optical cavity. The atoms are then let fallen down one by one through the cavity and if the MOT is distant enough from the cavity, and using appropriate collimators, the atom velocity is exactly orthogonal to the cavity axis x . We want to encode qubits into the CV corresponding to the atomic motion along x and the relevant dynamics is described (assuming, as usual in the optical domain, the rotating wave and dipole approximation) by the following Hamiltonian [9]

$$\hat{H} = \hbar\omega_0\hat{\sigma}_z + \frac{\hat{p}^2}{2M} + \hbar\omega_c\hat{c}^\dagger\hat{c} + \hbar g_0 (\hat{\sigma}^\dagger\hat{c} + \hat{c}^\dagger\hat{\sigma}) \cos k_c \hat{x}. \quad (5)$$

In this Hamiltonian $\hat{\sigma}_z = (\hat{\sigma}^\dagger\hat{\sigma} - \hat{\sigma}\hat{\sigma}^\dagger)/2$, $\hat{\sigma}, \hat{\sigma}^\dagger$ are the atomic spin-1/2 operators associated with the two internal levels whose transition is quasi-resonant with the optical cavity mode, \hat{x}, \hat{p} are the atomic center-of-mass position and

momentum operators along x , M is the atomic mass, $\omega_0 = 2\pi c/\lambda_0$ is the atomic transition frequency (c is the speed of light), \hat{c}, \hat{c}^\dagger are the cavity mode annihilation and creation operators, $\omega_c = ck_c = 2\pi c/\lambda_c$ is the cavity mode frequency, and g_0 is the atom-field coupling constant.

A ponderomotive interaction between the atom and the cavity mode is obtained in the dispersive limit in which the cavity mode is highly (red) detuned from the atomic transition. In this limit, the upper atomic level can be adiabatically eliminated and also the spontaneous emission from it can be neglected. In such a condition the atom always remains in its ground state and the resulting ponderomotive Hamiltonian is (in a frame rotating at the frequency ω_c)

$$\hat{H} = \frac{\hat{p}^2}{2M} - \frac{\hbar g_0^2}{\delta} \hat{c}^\dagger \hat{c} \cos^2 k_c \hat{x}, \quad (6)$$

where $\delta \equiv \omega_0 - \omega_c$ is the detuning. We then make a second assumption, the so called Raman-Nath approximation [9], which amounts to assume that the interaction time t (given by the time the atom takes to cross the cavity mode, i.e. $t \simeq 2w_0/v$, where w_0 is the cavity mode waist and v is the atom velocity) is short enough so that any variation of the atomic kinetic energy along x due to photon exchanges with the cavity field can be neglected. In this limit the kinetic energy along the cavity axis becomes a constant of motion, equal to its value before the cavity crossing, and therefore can be eliminated from the Hamiltonian of Eq. (6).

At the beginning the cavity mode is in a coherent state $|\alpha\rangle_c$ (we can always choose the phase reference so that $\alpha \geq 0$), while the atomic motion along the cavity axis x is described by a generic wave-function $\Phi(x)$, so that the initial state of the system is

$$|\Psi(0)\rangle = |\alpha\rangle_c \otimes \int dx \Phi(x) |x\rangle_a = \int dx \Phi(x) |\alpha, x\rangle. \quad (7)$$

At the end of the atom-cavity interaction, i.e. after the interaction time t , the state of the system becomes [9]

$$|\Psi(t)\rangle = e^{-\frac{i}{\hbar} \hat{H} t} |\Psi(0)\rangle = \int dx \Phi(x) |\alpha(x, t), x\rangle, \quad (8)$$

where

$$\alpha(x, t) = \alpha_1(x, t) + i\alpha_2(x, t) = \alpha \exp\left(i \frac{g_0^2 t}{\delta} \cos^2 k_c x\right). \quad (9)$$

Just at the end of the interaction we measure the intracavity quadrature $\hat{x}_0 = \hat{c} + \hat{c}^\dagger$ [14] obtaining the result x_0 . As a consequence the cavity mode is projected onto the corresponding quadrature eigenstate $|x_0\rangle$, while the atomic motion along x is disentangled from the cavity mode and it is projected onto the state with wave-function [9]

$$\Phi_{x_0}(x, t) = N_{x_0, t} \Phi(x) \exp\left\{-\left[\alpha_1(x, t) - \frac{x_0}{2}\right]^2 - i\alpha_2(x, t) [\alpha_1(x, t) - x_0]\right\}, \quad (10)$$

where $N_{x_0, t}$ is a normalization constant. Now it is possible to see that this state becomes a comb-like state with well localized spikes, so that it can be used as an approximate codeword, if we choose the interaction time t where we make the homodyne measurement such that $g_0^2 t / \delta = \pi$, and we take as initial wave-function $\Phi(x)$ a completely delocalized state, i.e.

$$\Phi(x) = \begin{cases} L^{-\frac{1}{2}} & 0 \leq x \leq L \\ 0 & x < 0, x > L \end{cases}, \quad (11)$$

which is an approximate momentum eigenstate with $p = 0$ (L is the cavity length). Such a delocalized state can be prepared using a suitable diverging atomic lens, i.e. an antinode of a blue-detuned cavity or another repulsive quadratic optical potential [13, 16], soon after the MOT and before the atom enters the cavity (see Fig. 2). With the above choices, the atomic wave-function of Eq. (10) takes the following form

$$\Phi_{x_0}(x) = \begin{cases} N_{x_0} \exp\{-[\alpha_1(x) - \frac{x_0}{2}]^2 - i\alpha_2(x) [\alpha_1(x) - x_0]\} & 0 \leq x \leq L \\ 0 & x < 0, x > L \end{cases} \quad (12)$$

where $\alpha_1(x)$ and $\alpha_2(x)$ are given by Eq. (9) with $g_0^2 t / \delta = \pi$ and the normalization constant N_{x_0} is given by

$$N_{x_0} = \sqrt{\frac{k_c}{d J(\alpha, x_0)}} \exp\left(\frac{x_0^2}{4}\right), \quad (13)$$

where $d = 2L/\lambda_c$ is the integer number of half-wavelengths of the stationary cavity mode and

$$J(\alpha, x_0) \equiv \int_0^\pi dy \exp \{2\alpha_1(y)[x_0 - \alpha_1(y)]\}. \quad (14)$$

The normalization factor is connected with the probability density of the outcome x_0 of the homodyne measurement, which is given by

$$\mathcal{P}(x_0) = \frac{J(\alpha, x_0)}{\sqrt{2\pi^3}} \exp \left(-\frac{x_0^2}{2} \right). \quad (15)$$

In order to make a direct comparison with the ideal codewords of Sec. II and to simplify the formulas, in the following we adopt dimensionless position and momentum operators by setting $\lambda_c = \hbar = 1$. It is also convenient to consider the scaled dimensionless position variable $y = k_c x$, as we have already done in Eq. (14) where $\alpha_1(y) = \alpha_1(x = y/k_c)$.

A. Homodyning with a zero outcome

For the sake of simplicity, we shall consider from now on the particular case of a homodyne measurement result, $x_0 = 0$. First of all we define the atomic state of Eq. (12) with $x_0 = 0$, as the approximate codeword $|\tilde{0}\rangle$, i.e.

$$\varphi_0(x) \equiv \langle x | \tilde{0} \rangle = \Phi_{x_0=0}(x) = N_0 \exp[-\alpha_1(x)^2 - i\alpha_1(x)\alpha_2(x)], \quad (0 \leq x \leq L) \quad (16)$$

where $N_0 \equiv N_{x_0=0}$. One can verify that the resulting wave-function $\varphi_0(y)$ is periodic in $0 \leq y \leq \pi d$ with period equal to π and it has $2d$ equally-spaced spikes (i.e. with $\pi/2$ -spacing, see Fig. 3(a)), so that its choice as approximate codeword state $|\tilde{0}\rangle$ is justified. From such a state it is easy to generate the associated codeword state $|\tilde{1}\rangle$ by simply displacing in y the state $|\tilde{0}\rangle$ by the quantity $\pi/4$, so that the corresponding wave-function is $\varphi_1(y) = \varphi_0(y - \pi/4)$ (which is nonzero in $\pi/4 \leq y \leq \pi d + \pi/4$, see Fig. 4 for a schematic description of the corresponding probability distributions). The practical implementation of the displacement of the atomic wave-function can be achieved by applying, just after the cavity, a suitable electric field gradient pulse with an appropriate intensity.

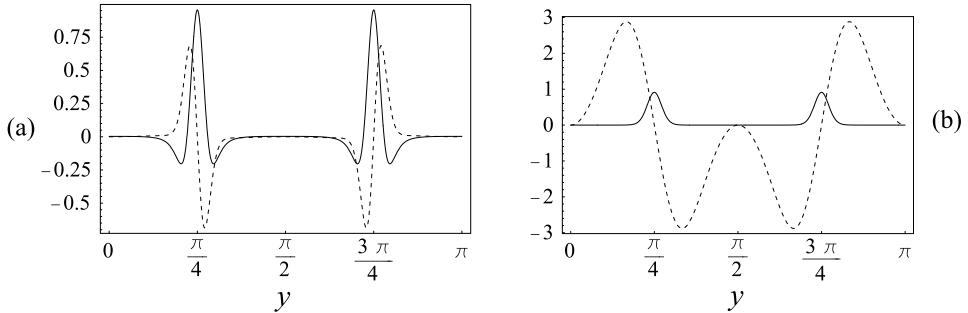


FIG. 3: Approximate codeword $|\tilde{0}\rangle$ corresponding to the parameters $\alpha = 2.4$ and $d = 20$. In (a) the real part of the spatial wave-function $\text{Re}\varphi_0$ (solid line) and the imaginary part $\text{Im}\varphi_0$ (dashed line) are plotted vs the scaled position variable y inside a single period. In (b) the spatial probability distribution $|\varphi_0|^2$ (solid line) and the phase $-i \ln[\varphi_0/|\varphi_0|]$ (dashed line) are plotted vs the scaled position variable y inside a single period.

After seeing how the two basis codeword states are generated, let us now see how to generate a generic superposition of the two, $a|\tilde{0}\rangle + b|\tilde{1}\rangle$. These superpositions can be generated using conditional displacement schemes analogous to those used, for example, in the manipulation of quantum states of trapped ions [17] and which exploit the coupling of a motional degree of freedom with an internal transition of the ion. Schematically these schemes proceed as follows. The atom is prepared in the tensor product state $|\tilde{0}\rangle \otimes [a|g\rangle + b|e\rangle]$, where $|e\rangle$ and $|g\rangle$ are two ground state sublevels. Then a laser pulse which is only coupled to $|e\rangle$ is applied to the atom and its intensity is tuned so to give exactly a position shift $y \rightarrow y - \pi/4$. In this way the state of the atom becomes $a|g\rangle \otimes |\tilde{0}\rangle + b|e\rangle \otimes |\tilde{1}\rangle$. Then a *rf pulse* resonant with the $e \rightarrow g$ transition and transforming $|e\rangle \rightarrow (|e\rangle + |g\rangle)/\sqrt{2}$ and $|g\rangle \rightarrow (|g\rangle - |e\rangle)/\sqrt{2}$ is applied, so that the state of the atom becomes $[(|g\rangle \otimes (a|\tilde{0}\rangle + b|\tilde{1}\rangle) + |e\rangle \otimes (b|\tilde{1}\rangle - a|\tilde{0}\rangle)]/\sqrt{2}$. When the internal state of the atom is measured and it is found equal to $|g\rangle$, the atomic motional state is conditionally generated in the desired encoded

superposition $a|\widetilde{0}\rangle + b|\widetilde{1}\rangle$. Examples of superposition states are also the approximate eigenstates $|\widetilde{\pm}\rangle$ of the phase-flip operator \bar{X} and equivalent set of codewords, which are given by $|\widetilde{\pm}\rangle \equiv [|\widetilde{0}\rangle \pm |\widetilde{1}\rangle]/\mathcal{N}_{\pm}$, where $\mathcal{N}_{\pm}^2 = 2(1 \pm \text{Re}[\langle \widetilde{0}|\widetilde{1}\rangle])$ because $|\widetilde{0}\rangle$ and $|\widetilde{1}\rangle$ are not exactly orthogonal in general. Their wave-function $\varphi_{\pm}(y) = [\varphi_0(y) \pm \varphi_1(y)]/\mathcal{N}_{\pm}$ are nonzero in $0 \leq y \leq \pi d + \pi/4$ and have spikes spaced by $\pi/4$. However these approximated codewords have to be close the ideal ones also in momentum space. Performing the Fourier transform of the above wave-functions, it is possible to see that the momentum wave-function of $|\widetilde{0}\rangle$ and $|\widetilde{1}\rangle$, $\psi_0(p)$ and $\psi_1(p)$, have equally spaced spikes separated by 8π , which coincide for even n and are opposite for odd n , due to the relation $\psi_0(p) = e^{ip/8}\psi_1(p)$, which is an immediate consequence of the translation by $\pi/4$ in the position coordinate. As a consequence, $\psi_{\pm}(p) = [\psi_0(p) \pm \psi_1(p)]/\mathcal{N}_{\pm}$ have spikes spaced by 16π and shifted by 8π with respect to each other (see Fig. 4 (b) for a schematic representation of the probability distributions in momentum space). Therefore, from these considerations, and comparing Fig. 4 with the description of the ideal codewords states in Fig. 1, we can conclude that the states generated in this lithographic scheme can certainly be used as approximated codeword states in the case of a spacing parameter $\theta = 1/8$ (see Eqs.(1)-(4)). In such a case in fact, the structure of the peaks is recovered both in position and momentum space for the four codewords, even though, as expected, the approximated codewords have a finite number of peaks ($2d$) and the peaks have a nonzero width and a finite height.

It is important to notice that, unfortunately, the codeword states generated in this way can be used only when the atoms are not too far from the cavity (*near field* regime). In fact, after leaving the cavity, the atomic motion along x evolves as a free particle and this evolution leads to quantum interference between the various spikes (see Ref. [9]). As we can see from Fig. 3(b), the phase change of the front of the atomic wave-function is approximately linear at the position y where $|\varphi_0(y)|^2 \neq 0$; for this reason, the various spikes are deflected after the cavity and they interfere in the *far field* [9].

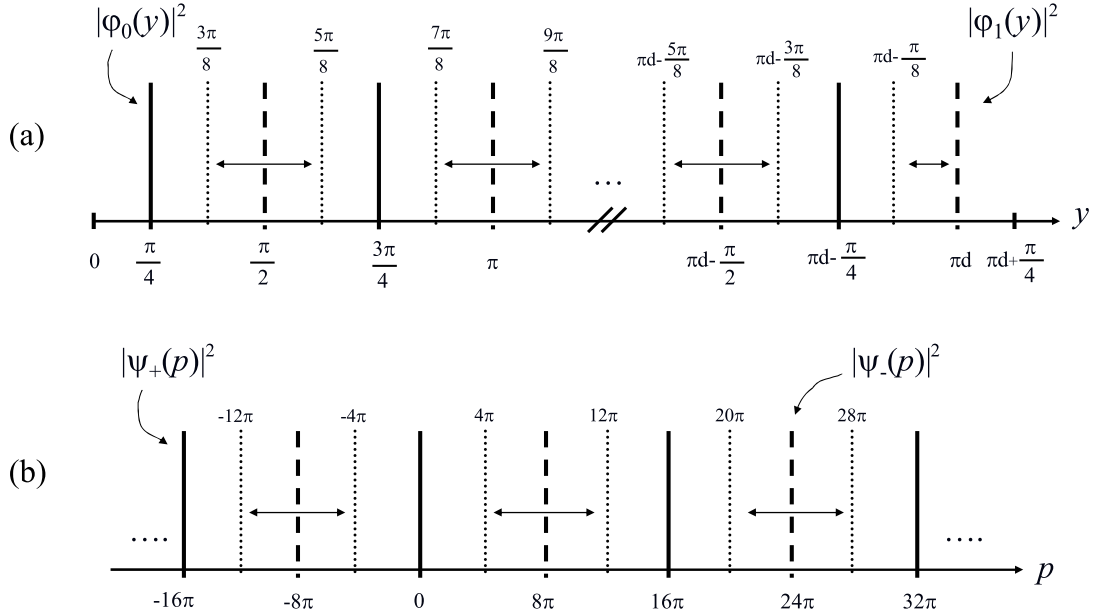


FIG. 4: (a) Structure of the spatial probability distributions $|\varphi_0|^2$ (solid lines), $|\varphi_1|^2$ (dashed lines) of the approximate codewords $|\widetilde{0}\rangle, |\widetilde{1}\rangle$ vs the scaled variable y . The two distributions are displaced by $\pi/4$ and each of them has $\pi/2$ -spaced spikes. Dotted lines and arrows delimit the error regions R_n, R_{2d} defined in the text. (b) Structure of the momentum probability distributions $|\psi_+(p)|^2$ (solid lines), $|\psi_-(p)|^2$ (dashed lines) of the approximate codewords $|\widetilde{+}\rangle, |\widetilde{-}\rangle$. The two distributions are displaced by 8π and each of them has 16π -spaced spikes. Dotted lines and arrows delimit the error regions R_n^+ defined in the text.

B. Intrinsic error probability

As discussed in Sec. II, when approximated codewords are used, one has additional errors (intrinsic errors). In fact, due to the presence of the tails of the peaks, the recovery process may lead sometimes to a wrong codeword. The recovery in the spatial variable is performed by measuring the operator $\hat{y}(\text{mod}\pi/4)$. We can see from Fig. 4 (a) that

an intrinsic error in the recovery process occurs when, given the state $\varphi_0(y)$, the measurement gives a result within one of the error regions: $R_n \equiv [(4n-1)(\pi/8), (4n+1)(\pi/8)]$, $n = 1, \dots, 2d-1$ and $R_{2d} \equiv [\pi d - \pi/8, \pi d]$. In such a case, in fact, the original state $|0\rangle$ will be correct to the other one $|1\rangle$ corrupting the encoded information even in the absence of any errors of the channel. The corresponding error probability $P_{x,0}$ is equal to the one, $P_{x,1}$, which we would obtain starting from the state $\varphi_1(y)$ and considering the complementary error region $[\pi/4, \pi d] \setminus \bigcup_{n=1,2d} R_n$. So, we simply have

$$P_x = \sum_{n=1}^{2d} \int_{R_n} \frac{dy}{2\pi} |\varphi_0(y)|^2 = \frac{(4d-1) N_0^2}{2\pi} \int_0^{\frac{\pi}{8}} dy \exp \left[-2\alpha_1(y)^2 \right]. \quad (17)$$

The recovery in momentum space is done by measuring the operator $\hat{p}(\text{mod}8\pi)$. In the same way, one can define (see Fig. 4 (b)) the two different error regions: $R_n^+ \equiv [(2n+1)8\pi - 4\pi, (2n+1)8\pi + 4\pi]$ and $R_n^- \equiv [(2n)8\pi - 4\pi, (2n)8\pi + 4\pi]$ with $n = 0, \pm 1, \dots$. An error in the recovery process occurs when, given the state $\psi_{\pm}(p)$, the measurement gives a result within one of the error regions R_n^{\pm} . The corresponding error probability is then given by

$$P_{p,\pm} = \sum_{n=-\infty}^{+\infty} \int_{R_n^{\pm}} dp |\psi_{\pm}(p)|^2 = \frac{2}{\mathcal{N}_{\pm}^2} \sum_{n=-\infty}^{+\infty} \int_{R_n^{\pm}} dp \left(1 \pm \cos \frac{p}{8} \right) |\psi_0(p)|^2. \quad (18)$$

Exploiting the parity of $|\psi_0(p)|^2$ and the inequality (true almost everywhere)

$$|\psi_0(p)|^2 \leq \frac{4N_0^2}{\pi} \frac{\sin^2(\frac{pL}{2})}{p^2}, \quad (19)$$

we obtain

$$P_{p,+} \leq \frac{16}{\pi} \frac{N_0^2}{\mathcal{N}_+^2} \sum_{n=0}^{+\infty} \int_{(4n+1)4\pi}^{(4n+3)4\pi} dp \left(1 + \cos \frac{p}{8} \right) \frac{\sin^2(pL/2)}{p^2} \equiv P_+, \quad (20)$$

and

$$P_{p,-} \leq \frac{8}{\pi} \frac{N_0^2}{\mathcal{N}_-^2} \left\{ \int_{-4\pi}^{4\pi} dp \left(1 - \cos \frac{p}{8} \right) \frac{\sin^2(pL/2)}{p^2} + 2 \sum_{n=1}^{+\infty} \int_{(4n-1)4\pi}^{(4n+1)4\pi} dp \left(1 - \cos \frac{p}{8} \right) \frac{\sin^2(pL/2)}{p^2} \right\} \equiv P_-. \quad (21)$$

To estimate the quality of the overall encoding procedure provided by our scheme, we have to consider a mean intrinsic error probability \bar{P}_e , which is obtained in general by averaging over all the possible encoded qubit states. Using the above definitions, we have that the mean intrinsic error probability \bar{P}_e satisfies the inequality

$$\bar{P}_e \lesssim \max \{P_x, P_{p,+}, P_{p,-}\} \leq \max \{P_x, P_+, P_-\} \equiv P_{\max}, \quad (22)$$

which defines the maximum intrinsic error probability P_{\max} , providing therefore a good characterization of the proposed encoding scheme.

We have therefore to estimate P_{\max} in the case of implementation on a realistic cavity QED apparatus (see for example Ref. [18]). In general the error probabilities $P_x, P_{p,\pm}$ depend on two dimensionless parameters: α , the amplitude of the initial coherent field in the cavity, and d , which is connected to the cavity length. These parameters cannot be taken at will however, because we have to satisfy the assumptions used for the derivation of the approximated codeword states, namely the large detuning and the Raman-Nath approximations. This latter approximation can also be expressed by imposing that the uncertainty of the position along the cavity axis acquired by the atom during the interaction time is much smaller than the cavity mode wavelength, i.e. $\Delta x \ll \lambda_c$ [9] (here, we re-introduce physical dimensions, in order to fully describe the experimental implementation). One has $\Delta p \simeq \alpha^2 \hbar k_c$ [9], from which we get $\Delta x \simeq \Delta p t / 2M \simeq \alpha^2 \hbar k_c t / 2M$, so that the Raman-Nath approximation implies the following condition on the interaction time

$$t \ll \frac{M \lambda_c^2}{\pi \hbar \alpha^2}. \quad (23)$$

On the other hand, the condition of large detuning implies $4\alpha^2 g_0^2 / \delta^2 \ll 1$ which, together with the condition $g_0^2 t / \delta = \pi$ used above, leads to another condition on the interaction time, i.e.

$$t \gtrsim \frac{2\pi\alpha}{g_0}, \quad (24)$$

which, combined with Eq. (23), gives the following bounds for the interaction time

$$\frac{2\pi\alpha}{g_0} \lesssim t \ll \frac{M\lambda_c^2}{\pi\hbar\alpha^2}. \quad (25)$$

This condition however puts also limitations on the possible values of α and of the coupling constant g_0 , which is related to the cavity mode volume V (and therefore to d because it is $V \sim \pi w_0^2 L = \pi w_0^2 d \lambda_c / 2$) by the relation $g_0 = d_{12} \sqrt{\omega_c / 2\hbar\varepsilon_0 V}$, where d_{12} is the electric dipole matrix element associated to the atomic transition and ε_0 is the vacuum dielectric constant. In order to satisfy Eq. (25) one can impose, for example, $2\pi\alpha/g_0 = 10^{-2} M\lambda_c^2 / \pi\hbar\alpha^2$ which becomes therefore an effective relation between the two apparently independent parameters α and d , which reads

$$\alpha = \sqrt[3]{\frac{g_0}{D}}, \quad D \equiv 10^2 \frac{2\pi^2\hbar}{M\lambda_c^2}. \quad (26)$$

To state it in other words, the assumptions made in order to derive the desired encoded states implies that in practice we have only *one* free parameter, which can be α , d or the coupling constant g_0 .

To show the experimental feasibility of the present scheme, we have considered the case of an heavy atom (Cs) and we have studied the behavior of the error probabilities P_x, P_{\pm} in the case of realistic parameters. In particular, we have considered $\lambda_0 = \lambda_c = 852.1$ nm and $d_{12} = 3.79 \times 10^{-29}$ Cm, so that $D \simeq 1.3 \times 10^6$ Hz. In Fig. 5 we have plotted the three error probabilities and the corresponding maximum probability P_{max} as a function of the coupling constant g_0 in the case of a cavity mode waist $w_0 = 20\mu\text{m}$. We can see that the error probabilities in position and in momentum behave in the opposite way for increasing g_0 and, for this reason, the upper bound P_{max} has a minimum at an intermediate value $g_0 \simeq 16$ MHz, where all the probabilities P_x, P_{\pm} have about the same order of magnitude, i.e. $\sim 10^{-4}$, which represents a remarkably small value of the intrinsic error probability. In such a case, we have $\alpha \simeq 2.3$, which gives $\mathcal{P}(x_0 = 0) \simeq 4.6\%$, while the interaction time is $t \simeq 3\mu\text{s}$, and the atom velocity is $v = 2w_0/t \simeq 40 \text{ ms}^{-1}$.

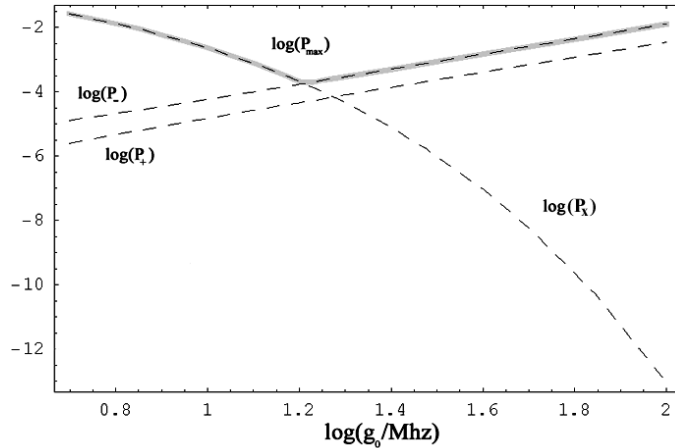


FIG. 5: $\log_{10}(P_x)$ and $\log_{10}(P_{\pm})$ (dashed-lines) versus $\log_{10}(g_0/\text{MHz})$ in the case of Cs and for a cavity waist $w_0 = 20\mu\text{m}$. The quantity $\log_{10}(P_{max})$ is the marked upper curve and it displays a minimum at about $g_0 = 16\text{MHz}$. In correspondence of such a minimum we have a mean error probability $\bar{P}_e \lesssim P_{max} \sim 2 \times 10^{-4}$.

IV. CONCLUSION

Continuous variable QEC consists in encoding quantum information (i.e. a qubit) into a quantum system whose state is described by observables with a continuous spectrum of eigenvalues. The redundancy of these CV degrees of freedom can be used to correct the errors which arise from the unwanted interactions with the environment, and therefore to safely protect the encoded quantum information. However, there is a *fault* in the CV QEC theory that concerns the physical generation of the CV quantum codewords which, ideally, are non-normalizable states. In other words, every real experimental setup can only make use of an approximate version of such codewords, and it comes out the problem of how one can generate such codewords and what are the consequent effects in terms of error correcting performances. Here, to face the problem, we have resorted to lithographic techniques. In particular, we have shown

how an optical cavity subjected to a homodyne measurement acts as a virtual diffraction grating which is able to project the motional state of a crossing neutral atom into a well-approximated quantum codeword. Actually, this CV encoding is limited in space, i.e., the generated CV quantum codewords will live only in the near-field regime, since they will be destroyed in the far-field regime due to quantum diffraction. However, under these assumptions, we have shown that sufficiently low values of the intrinsic error probability are effectively reachable (in particular $\sim 10^{-4}$ using a Cesium atom).

[1] See e.g. *Quantum Information Theory with Continuous Variables*, edited by A. K. Pati and S. L. Braunstein, Kluwer Academic Press (2002).

[2] S. Braunstein, Phys. Rev. Lett. **80**, 4084 (1998); S. Lloyd and J. E. Slotine, Phys. Rev. Lett. **80**, 4088 (1998).

[3] D. Gottesman, A. Kitaev, and J. Preskill, Phys. Rev. A **64**, 012310 (2001).

[4] B. C. Travaglione and G. J. Milburn, Phys. Rev. A **66**, 052322 (2002).

[5] B. C. Travaglione and G. J. Milburn, Phys. Rev. A **65**, 032310 (2002).

[6] S. Pirandola, S. Mancini, D. Vitali and P. Tombesi, Europhys. Lett. **68**, 323 (2004).

[7] S. Pirandola, S. Mancini, D. Vitali and P. Tombesi, quant-ph/0503003 (accepted for publication on EPJD).

[8] S. Mancini and P. Tombesi, Phys. Rev. A **49**, 4055 (1994).

[9] P. Storey, M. Collett, and D. F. Walls, Phys. Rev. Lett. **68**, 472 (1992).

[10] D. F. Walls, Aust. J. Phys. **49**, 715 (1996).

[11] A one-dimensional quantum oscillator or a one-dimensional free particle, which is a 1 – dim quantum oscillator with zero frequency.

[12] D. Gottesman, Phys. Rev. A **54**, 1862 (1996); A. R. Calderbank, E. M. Rains, P. W. Shor, and N. J. A. Sloane, Phys. Rev. Lett. **78**, 405 (1997).

[13] H. J. Metcalf and P. van der Straten, *Laser Cooling and Trapping* (Springer, 1999).

[14] It is possible to make a direct and precise measurement of this intracavity quantity using a high finesse cavity whose input-output mirror transmittivity is controlled through fast electronics [15].

[15] M. S. Taubman, H. M. Wiseman, D. E. McClelland, and H. A. Bachor, J. Opt. Soc. Am. B **12**, 1792 (1995).

[16] J. Bjorkholm, R. Freeman, A. Ashkin, and D. Pearson, Phys. Rev. Lett. **41**, 1361 (1978).

[17] D. Leibfried, R. Blatt, C. Monroe, and D. Wineland Rev. Mod. Phys. **75**, 281 (2003).

[18] J. McKeever, J. R. Buck, A. D. Boozer, A. Kuzmich, H.-C. Nagerl, D. M. Stamper-Kurn, and H. J. Kimble Phys. Rev. Lett. **90**, 133602 (2003).